



# Antimicrobial activity of phenyllactic acid against *Klebsiella pneumoniae* and its effect on cell wall membrane and genomic DNA

Jianyun Yu<sup>1</sup> · Chunli Hong<sup>1</sup> · Longfei Yin<sup>1</sup> · Qingbo Ping<sup>1</sup> · Gaowei Hu<sup>1</sup>

Received: 18 July 2023 / Accepted: 9 September 2023 / Published online: 20 September 2023  
© The Author(s) under exclusive licence to Sociedade Brasileira de Microbiologia 2023

## Abstract

As *Klebsiella pneumoniae* (KP) has acquired high levels of resistance to multiple antibiotics, it is considered a worldwide pathogen of concern, and substitutes for traditional antibiotics are urgently needed. 3-Phenyllactic acid (PLA) has been reported to have antimicrobial activity against food-borne bacteria. However, there was no experiment evidence for the exact antibacterial effect and mechanism of PLA kills pathogenic KP. In this study, the Oxford cup method indicated that PLA is effective to KP with a minimum inhibitory concentration of 2.5 mg/mL. Furthermore, PLA inhibited the growth and biofilm formation of in a time- and concentration-dependent manner. *In vivo*, PLA could significantly increase the survival rate of infected mice and reduce the pathological tissue damage. The antibacterial mode of PLA against KP was further explored. Firstly, scanning electron microscopy illustrated the disruption of cellular ultrastructure caused by PLA. Secondly, measurement of leaked alkaline phosphatase demonstrated that PLA disrupted the cell wall integrity of KP and flow cytometry analysis with propidium iodide staining suggested that PLA damaged the cell membrane integrity. Finally, the results of fluorescence spectroscopy and agarose gel electrophoresis demonstrated that PLA bound to genomic DNA and initiated its degradation. The anti-KP mode of action of PLA was attributed to the destruction of the cell wall, membrane, and genomic DNA binding. These findings suggest that PLA has great potential applications as antibiotic substitutes in feed additives against KP infection in animals.

**Keywords** Phenyllactic acid · Antibacterial activity and mechanism · Cell wall membrane integrity · Genomic DNA

## Introduction

*Klebsiella pneumoniae* (KP) is a Gram-negative opportunistic pathogen belonging to the family *Enterobacteriaceae* [1]. Infections have been reported in humans, livestock, poultry, and aquatic animals, mainly causing respiratory tract infection, urinary tract infection (UTI), and even sepsis [2–6]. Therefore, diseases caused by KP pose a great threat to human and animal health.

Antibiotics are the first choice for antibacterial therapy, but the advent of extended-spectrum  $\beta$ -lactamase

(ESBL)-producing KP had led to increasing therapeutic failure with many clinical antibiotics, such as aminoglycosides, sulfamethoxazole, tetracyclines, fluoroquinolones, and trimethoprim [3]. However, the antimicrobial resistance varies with the different strains, host species, antimicrobial concentrations, growth conditions, and genetic traits [7–9]. Due to its resistance to multiple antibiotics, KP infection requires extremely difficult treatment, and there is an increase of mortality, which has become a major concern around the world [10]. In this context, novel therapeutic options that are effective against KP are urgently needed [11].

3-Phenyllactic acid (PLA) is produced by many lactic acid bacteria and shows antimicrobial activity against a broad spectrum of bacteria, including *Listeria monocytogenes*, *Escherichia coli*, *Enterococcus faecalis*, and *Enterobacter cloacae*, as well as some fungi, yeasts, and molds [12–14]. Although the antibacterial effect of PLA has been reported, previous studies mainly focused on the antibacterial activity of PLA *in vitro* [12, 13, 15]. In addition, the existing antibacterial mechanism of PLA was explored the

---

Responsible Editor: David Germano Gonçalves

✉ Gaowei Hu  
hugaowei68@163.com

<sup>1</sup> College of Life Sciences, Taizhou key Laboratory of Biomass Functional Materials Development and Application, Taizhou University, Taizhou, Zhejiang 318000, China

membrane permeability leading to the leakage of intracellular components [12, 16]. However, there is no experimental evidence for the mechanisms underlying the antibacterial activity of PLA against pathogens KP *in vivo* and its effect mechanism.

Therefore, the present study aimed to explore the *in vitro* antibacterial effect of PLA against KP and, importantly, to evaluate PLA protection in mouse infection model and elucidate its antimicrobial mode. In detail, the changes in morphology, cell wall membrane, and genomic DNA were monitored after treatment with PLA.

## Materials and methods

### Chemicals and bacterial strains

PLA ( $\geq 98\%$ ) was purchased from sigma (Saint Louis, MO, USA). *Klebsiella pneumoniae* KPLYC2 (identified by 16sRNA, GenBank: MT953921) was isolated from a diseased large yellow croaker fish (*Larimichthys crocea*) and has tetracycline resistance and  $\beta$ -lactam antibiotic resistance [17]. Strain CVCC4080 (the infected host is mammal) was purchased from China Institute of Veterinary Drug Control (Beijing, China) and has  $\beta$ -lactam antibiotic resistance and quinolones resistance [9, 17]. Strain ATCC700603 (standard strain) was stored in our laboratory and includes  $\beta$ -lactam antibiotic resistance and carbapenem-resistance [18, 19]. Strain CVCC4080 was used for infection in the mouse model.

Bacteria were streaked from glycerol cryostocks onto LB plates and incubated overnight at 37 °C. A single bacterial colony from the fresh plate was used to inoculate LB broth and grown at 37 °C in a shaking incubator at 180 rpm to an  $OD_{600}$  of 0.6, which corresponds to  $2.5 \times 10^8$  colony forming units (CFU)/mL, as confirmed by plating 10-fold serial gradient dilutions.

### Antibacterial susceptibility assay using the Oxford cup method

The PLA and kanamycin (used as control) at a concentration of 100  $\mu\text{g}/\text{mL}$  were co-incubated with 3 strains to detect their antibacterial activity using the Oxford cup method [20]. The diameter of the inhibition zone was measured to determine the antibacterial activity of PLA against KP. An equal volume of sterile water was used as the negative control.

### Minimal inhibitory concentrations (MIC) and minimum bactericidal concentrations (MBC)

The determination of MIC and MBC of PLA was adapted from a previous study [21] with minor modifications as

follows. Briefly,  $1 \times 10^6$  CFU/mL of KP was added to 500  $\mu\text{L}$  of LB liquid medium containing PLA at concentrations ranging from 0 to 10 mg/mL. The LB liquid medium with bacteria without any PLA was used as the negative control. All the cultures were incubated at 37 °C for 24 h, after which 200  $\mu\text{L}$  were transferred into the 96-well plates, and the optical density (OD) of each well was recorded at 600 nm using a microplate reader (InfinteF200Pro, Tecan, Switzerland). Sterile LB with PLA was used as the blank control. The MIC was defined as the lowest PLA concentration that inhibited the growth of KP. MBC was measured by subculturing the broths used for MIC determination on fresh agar plates. The MBC was defined as the lowest PLA concentration that results in 99.9% cell death of the KP strain, or less than 3 CFU surviving [22]. All the experiments were conducted in triplicate.

### Time-dependent bactericidal activity

Time-dependent bactericidal activity was analyzed using the plate colony count method according to a previous study [23]. KP was incubated at 37 °C and 180 rpm in LB containing PLA at a concentration of  $1 \times \text{MIC}$  at a final concentration of  $1 \times 10^6$  CFU/mL. Then, aliquots were collected to perform colony counting every 4 h for 24 h. The number of viable cells was quantified by plating ten-fold serial dilutions for each sample at desired time points and counting colonies after incubation at 37 °C for 24 h. The growth curves of bacteria were drawn by plotting the mean colony counts (Lg CFU/mL) versus time.

### Biofilm formation assay

The inhibition of KP biofilm formation by PLA was tested using the crystal violet biofilm assay in 96-well microplates as previously described [24, 25], with minor modifications as follows. Briefly,  $1 \times 10^6$  CFU/mL of KP cells was inoculated into 96-well plates and incubated with different concentrations of PLA (0,  $0.5 \times \text{MIC}$ ,  $1 \times \text{MIC}$ ) at 37 °C. At the indicated time points (12, 24, and 36 h), the cultures were washed 3 times with PBS to remove all planktonic cells. To quantify biofilm density, the plates were then air-dried for 5 min at room temperature and stained with 0.1% crystal violet for 15 min, and the excess dye was removed by washing 2 times with PBS. Then, the wells were incubated with 150  $\mu\text{L}$  of 95% ethanol. After incubation, 100  $\mu\text{L}$  of the destaining solution was transferred to a new plate, and the absorbance at 570 nm ( $A_{570}$ ) was measured. The specific biofilm formation rate was calculated by comparing the  $A_{570}$  [26].

## Mouse infection model and treatment

All animal experiments followed the guidelines of the Institutional Animal Care and Use Committee of Taizhou University and were approved by the Committee (Approval No. TZXY-2022-20221046). Six-week-old female BALB/c mice ( $20 \pm 1.5$  g) were purchased from Shanghai SLAC Laboratory Animal Co., Ltd, China. They were kept at room temperature with free access to food and water. Groups of 15 mice were infected with  $2 \times 10^6$  CFU of strain CVCC4080 via the intraperitoneal (ip) route. Then, the mice were mock-treated with normal saline (NS, negative control) or PLA (treatment group, prepared 2.5 mg/mL of PLA and each mouse was given 0.2 mL) by gavage 12 h post-infection, which was continued twice a day every 8 h for 10 days. The survival rates of the mice were recorded for 15 days to plot survival curves, which were used to assess the therapeutic efficacy of PLA.

## Histopathological examination

To evaluate the amelioration of pathological damage in mice by PLA, the livers, lungs, and small intestine of 5 mice from each group were collected at 7 days post-infection (dpi) and fixed by immersion in 4% paraformaldehyde. The fixed tissues were sent to a company (Pinuofei Biotechnology Co., Ltd, Wuhan, China) for HE staining and imaging analysis.

## Scanning electron microscopy (SEM)

The morphological changes of KP bacterial cells were observed by SEM according to a previous study [25]. KP cells at a density of  $1.0 \times 10^6$  CFU/mL in LB were incubated with NS, 1  $\times$  MIC and 2  $\times$  MIC PLA. After incubation at 37 °C for 1, 2, and 4 h, the cells were collected by centrifugation and fixed with 2.5% glutaraldehyde overnight at 4 °C. The fixed cells were washed with PBS 3 times, dehydrated with a gradient of aqueous ethanol solutions (30%, 50%, 70%, 80%, 90%, and 100%), treated with isoamyl acetate 2 times, and then lyophilized. Finally, the dried cells were fixed onto a copper net and sputter-coated with gold under vacuum before observation under a S-4800 SEM (Hitachi High-Technologies, Tokyo, Japan).

## Cell wall integrity assay

The integrity of the cell wall was determined by measuring the leaked extracellular AKP activity [27]. The bacterial cells were washed with PBS 3 times and then re-suspended. Then, PLA was added to a final concentration of 0.5  $\times$  MIC and 1  $\times$  MIC, while a corresponding volume of sterile water was used as the negative control. The cultures were incubated at 37 °C for 0, 10, 20, and 30 min, after

which 0.2 mL was passed through a 0.22- $\mu$ m pore-size filter membrane and added to 1.8 mL Tris-HCl buffer (pH = 8.0, 0.1 mol/L, containing 0.2 g/L 4-nitrophenyl phosphate disodium salt). Subsequently, the mixtures were incubated at 25 °C for 30 min. Finally, the absorbance at 410 nm was measured to calculate the amount of AKP in the solution.

## Membrane permeability analysis using PI staining

The impact of PLA on the cell membrane integrity was determined by fluorescence microscopy and flow cytometry according to published methods [13, 24]. Firstly,  $1 \times 10^4$  CFU/mL of KP cells were treated with 0, 1  $\times$  MIC, and 2  $\times$  MIC of PLA at 37 °C for 0.5, 1, and 2 h. After incubation, the cells were harvested by centrifugation and washed 3 times with PBS. Then, the cells were stained with PI (final concentration 10  $\mu$ g/mL) at 4 °C for 20 min in the dark, collected and rinsed with 0.1 M PBS to remove excess dye. Finally, the dead cells with red fluorescence were imaged by fluorescence microscopy (DMLS, Leica, Australia) and quantified using a FACScan Flow Cytometer (CytoFLEX S, Beckman Coulter, USA).

## The binding of PLA to bacterial genomic DNA

Competitive binding of PLA and nucleic acid dye (Sangon Biotech, co., LTD, China) to bacterial genomic DNA was confirmed by fluorescence spectrometry (Hitachi High-Technologies, Tokyo, Japan) according to a previous study [13]. Briefly, genomic DNA of KP was extracted using a Rapid Bacterial Genomic DNA Isolation Kit (Sangon Biotech, co., LTD, China) according to the operation manual. The purity and concentration of the extracted genomic DNA were determined by measuring the absorbance at 260 and 280 nm using an Evolution 220 Spectrophotometer (Thermo Scientific, USA). PLA with different concentrations (0, 0.5  $\times$ , 1  $\times$ , and 2  $\times$  MIC) was added to the genomic DNA (60 mg/L) and incubated at 37 °C for 15 min in the dark. The fluorescence of the mixture was measured using an F97Pro instrument (Shanghai Lengguang Technology, China) with an excitation wavelength of 560 nm and emission scanning in the range of 530–600 nm with a slit width of 10 nm. The degradation of DNA induced by PLA was confirmed by agarose gel electrophoresis. Briefly, bacterial genomic DNA was dissolved in TE buffer to a final concentration of 60 mg/L, and PLA solutions (0, 0.5  $\times$  and 1  $\times$  MIC) were added to the DNA and incubated at 37 °C in the dark for 15 min. After electrophoresis, the gel was observed and imaged using a gel imaging system (FR-980B Gel Image Analysis System, Shanghai Furi, China).

## Statistical analysis

All experiments were conducted in triplicate, and the results are expressed as the means  $\pm$  standard deviation. Graphs were made using GraphPad Prism Version 5 for windows (GraphPad Software, San Diego, CA, USA), and statistical analysis was conducted using SPSS 22.0 software (IBM Corp., Armonk, NY, USA). The statistical significance of differences in KP biofilm formation, survival rate, and flow cytometry data was determined using ANOVA followed by the least significant difference (LSD) test. Differences were considered statistically significant at  $P < 0.05$ . An asterisk (\*) indicates  $P < 0.05$  and two asterisks (\*\*) indicate  $P < 0.01$ .

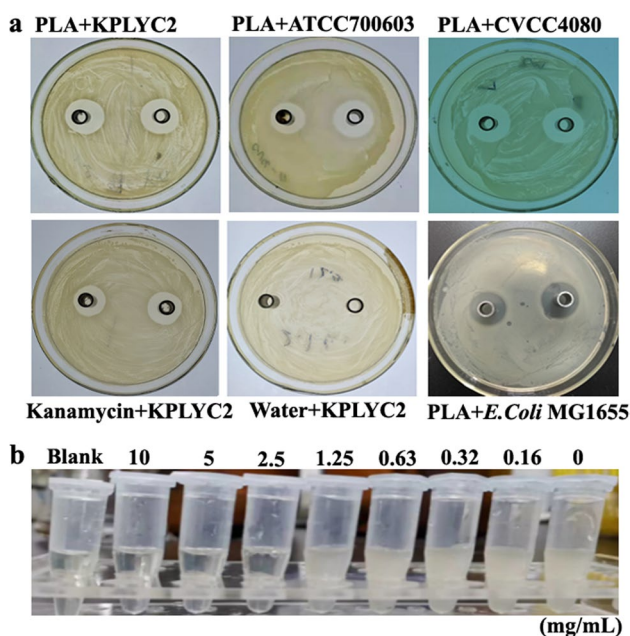


**Fig. 1** Inhibition zone of PLA against the 3 KP strains and MIC assay. **a** Determination of the inhibitory zone diameter of PLA against 3 strains of KP. An aliquot comprising 200  $\mu$ L of PLA at the indicated concentration was added to the Oxford cup and incubated with  $1 \times 10^6$  CFU/mL KP for 24 h. An equal volume of sterile water and kanamycin was used as the negative and positive control, respectively. **b** MIC assay. KP at a density of  $1 \times 10^6$  CFU/mL was incubated with PLA at concentrations of 10.00, 5.00, 2.50, 1.25, 0.63, 0.32, 0.16, and 0 g/L for 24 h. Then, 200  $\mu$ L of each culture was transferred into the 96-well plate and the optical density at 600 nm ( $OD_{600}$ ) of each well was determined

**Table 1** Inhibition zone, MIC, and MBC of PLA against 3 strains of KP

Groups	KPLYC2	ATCC700603	CVCC4080	Kanamycin	Water
Inhibition zone (mm)	21 $\pm$ 1	19.7 $\pm$ 1	22 $\pm$ 1	20 $\pm$ 1	NA
MIC (mg/mL)	2.5	2.5	2.5	-	-
MBC (mg/mL)	2.5	2.5	2.5	-	-

NA not available

## Results

### PLA inhibited the growth of KP

As shown in Fig. 1a, PLA exhibited an obvious antibacterial effect against KP, with mean inhibition zone (IZ) sizes of 21, 19.7, and 22 mm, which was similar to kanamycin with 20 mm. This result suggested that PLA could inhibit the growth of KP and produce the obvious inhibition zone. In Table 1, the  $OD_{600}$  measurements and microdilution assay demonstrated that the MIC and MBC of KP were 2.5 mg/mL.

### The antibacterial effect of PLA on KP was time-dependent

A survival curve was plotted to assess the time-dependent inhibitory effect of PLA on the growth of KP as shown in Fig. 2. The number of viable bacteria continually increased without PLA as expected. By contrast, all 3 strains displayed a reduction of viability when exposed to PLA at their corresponding  $1 \times \text{MIC}$  after 4 h of growth, confirming the inhibitory effect of PLA against KP. Moreover, the growth of KP bacteria decreased more obviously with prolonged treatment time.

### PLA inhibited biofilm formation in KP

The biofilm formation process of strain CVCC4080 was assessed using crystal violet staining. As shown in Fig. 3, the biofilm of untreated KP obviously increased from 12 to 36 h of cultivation, and biofilm formation was significantly reduced by PLA at  $0.5 \times \text{MIC}$  and  $1 \times \text{MIC}$  at all tested time-points ( $P < 0.01$ ). Thus, the results confirmed that PLA could inhibit bacterial growth and biofilm formation in KP strain CVCC4080.

### Efficacy of PLA against KP infection in a mouse model

Mice were infected with  $2 \times 10^6$  CFU of strain CVCC4080 and gavaged with NS or PLA for 10 days. While all mice in the NS group after KP infection died within 7 days (Fig. 4), 93% of the mice in the PLA group survived until 10 dpi, and the survival rate decreased to 74% at 11 dpi. Overall, 56%

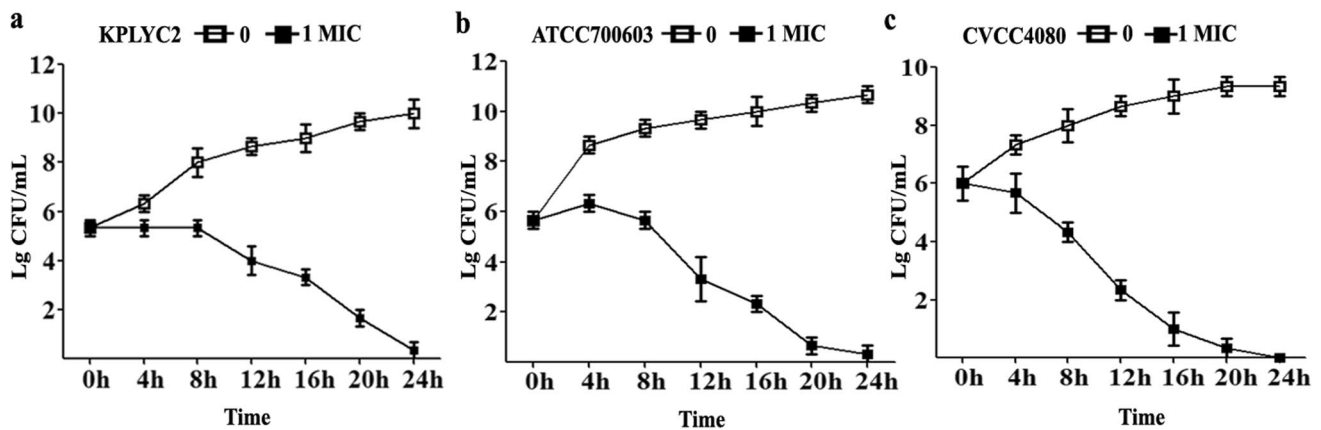


**Fig. 2** Time-dependent reduction in the viability of 3 strains of KP following treatment with PLA. The KP cells were added at a final concentration of  $1 \times 10^6$  CFU/mL to LB containing PLA at the con-

centration of  $1 \times \text{MIC}$  and incubated at  $37^\circ\text{C}$  under constant shaking. Aliquots were collected to perform colony counting every 4 h for 24 h

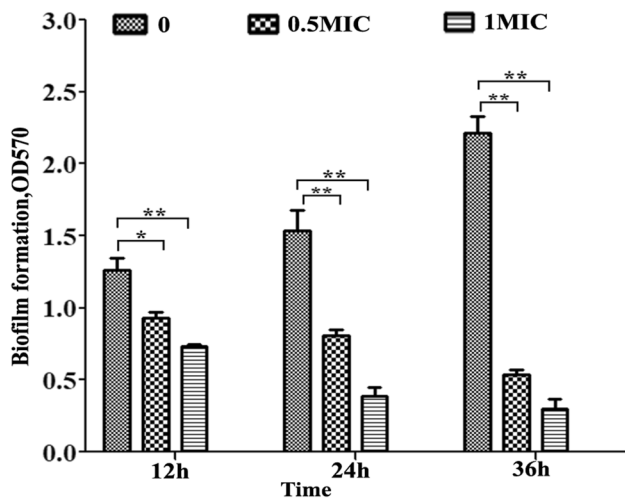


**Fig. 3** Effect of PLA on KP biofilm formation. KP cells at a density of  $1 \times 10^6$  CFU/mL were incubated with different concentrations of PLA in 96-well plates for 12, 24, and 36 h. The biofilms were stained with 0.1% crystal violet, and the absorbance was determined at 570 nm. The data were expressed as means  $\pm$  standard deviations ( $n = 3$ ) \* $P < 0.05$ ; \*\* $P < 0.01$

of mice treated with PLA survived the lethal challenge with KP through injection (Fig. 4).

### PLA ameliorated the histopathological injury caused by KP

The lung, liver, and small intestine tissues were fixed and sectioned for histopathological examination. As shown in Fig. 5, liver sections from the NS group mice after KP infection exhibited obvious diffuse hemorrhage, inflammatory cell infiltration, and hyperemia (Fig. 5a). In addition to obvious pathological changes, such as diffuse hemorrhage,

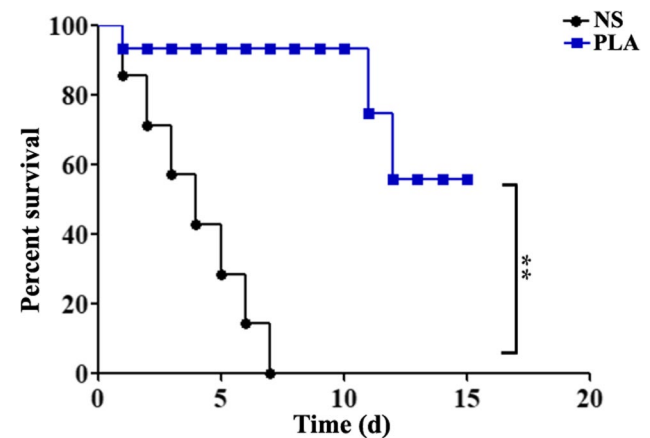


**Fig. 4** Therapeutic efficacies of PLA against infection with KP strain CVCC4080. The mice were infected with  $2 \times 10^6$  CFU of strain CVCC4080 via the ip route and then treated with NS or PLA by intragastric administration. Survival was recorded daily for 15 days ( $n = 10$ ). \*\* $P < 0.01$

destroyed alveoli, decreased number of alveoli, and thickened alveolar septa, the destruction of intestinal villus structure and inflammatory cell infiltration were observed in lung and small intestine tissues of mice from the NS group (Fig. 5b and c). Conversely, treatment with PLA greatly reduced these pathological changes (Fig. 5d-f).

### PLA treatment damaged the cellular ultrastructure

The morphological and ultrastructural changes of bacterial cells treated with PLA were observed by SEM (Fig. 6). The untreated KP cells displayed an obvious rod-shaped morphology with a smooth and regular surface, and the cells were uniform in size and distribution. By contrast, the cells treated with PLA exhibited a rounded shape with irregular

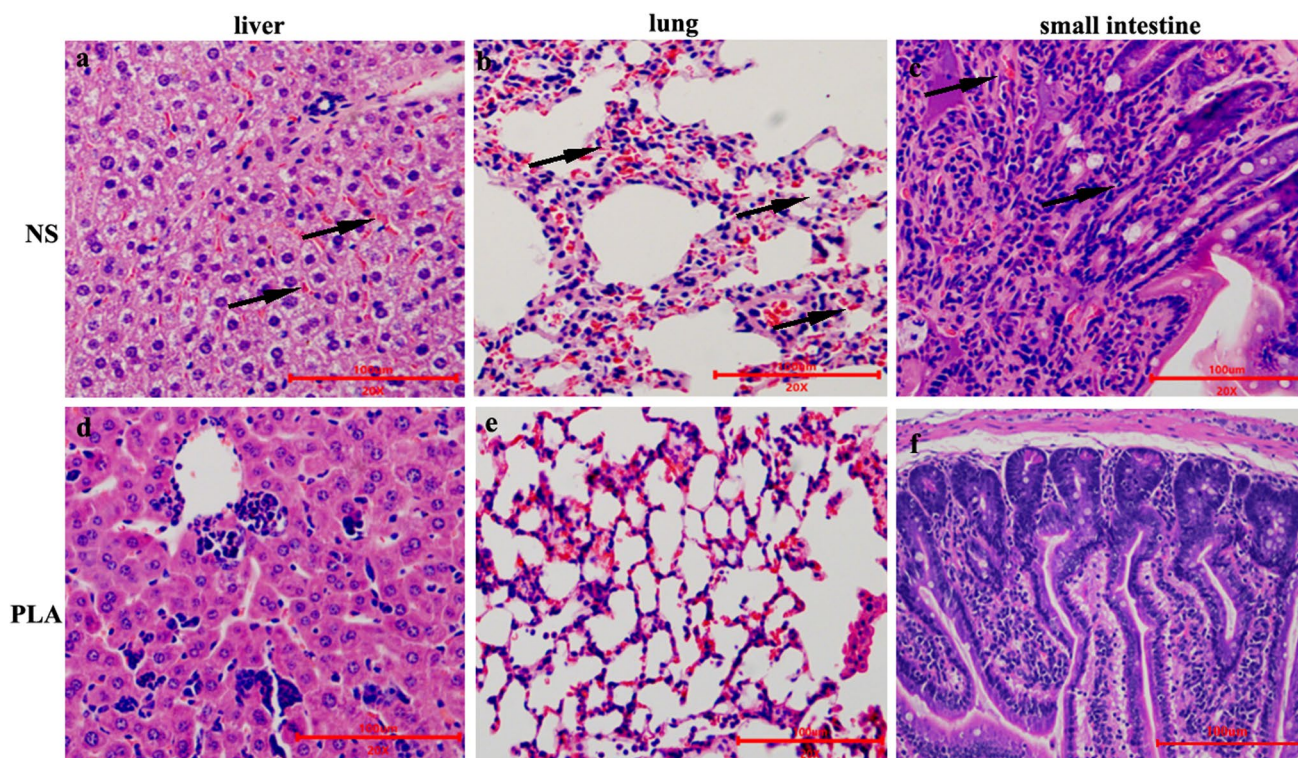


**Fig. 5** Effects of PLA treatment on the damage induced in the liver, lungs, and small intestines of mice by KP infection. **a–c** The liver, lungs, and small intestine of infected mice treated with NS were analyzed by histochemistry at 7 dpi. The arrow indicates diffuse hemorrhage, inflammatory cell infiltration and hyperemia, destroyed alveoli,

decreased number of alveoli, thickened alveolar septa, and destruction of intestinal villus structure. The sections were stained with H&E. **d–f** The liver, lungs and small intestine of infected mice treated with PLA were examined in the same way. Scale bars = 100  $\mu$ m

wrinkles, with pores or local ruptures formed on the cell surface, and with the further treatment time, large depressions, and cavities appeared. In addition, these changes became more obvious with the increase of PLA concentration and time. However, the basic murein structure of bacterial cells was still retained after exposure to PLA.

### PLA damaged the cell wall integrity of KP

Cell wall damage can be determined by the leakage of intracellular AKP into the culture supernatant. As presented in Fig. 7, the extracellular AKP from KP indicated by the  $OD_{410}$  value remained basically constant in the control group (approximately 0.13). However, this value increased dramatically after KP cells were treated with PLA. Furthermore, the release of AKP enzyme from KP cells was further enhanced with the increase of PLA concentration from 0.5 to 1  $\times$  MIC. Specifically, the mean  $A_{410}$  value of the substrate used to measure extracellular AKP in KP cell supernatant was increased from 0.13 to 0.52 and 0.84 in response to treatment with 0.5  $\times$  and 1  $\times$  MIC of PLA for 30 min, respectively. This result indicated that PLA damaged the cell

wall by disrupting its integrity, which resulted in the leakage of intracellular AKP into the cell supernatant.

### PLA increased the cell membrane permeability of KP

Cell membrane integrity of KP was assessed by propidium iodide (PI) staining. Propidium iodide exhibits a fluorescence signal when it binds to DNA. Viable cells with intact membrane integrity exclude PI from their DNA, and therefore do not produce fluorescence, whereas nonviable cells with a compromised membrane present a red fluorescence signal after staining with PI. As shown in Fig. 8, untreated KP cells emitted a negligible red fluorescence, confirming the physical integrity of their cell membrane. By contrast, when cells were treated with 1  $\times$  MIC of PLA, there was a marked increase of red fluorescence. At a dose of 2  $\times$  MIC, PLA treatment resulted in a significant increase of red fluorescence intensity, so that most KP cells were marked red, and it was evident that (Fig. 8a), suggesting that high concentration of PLA rapidly disrupted the integrity of the cell membrane. Based on the results of flow cytometry, 17% of

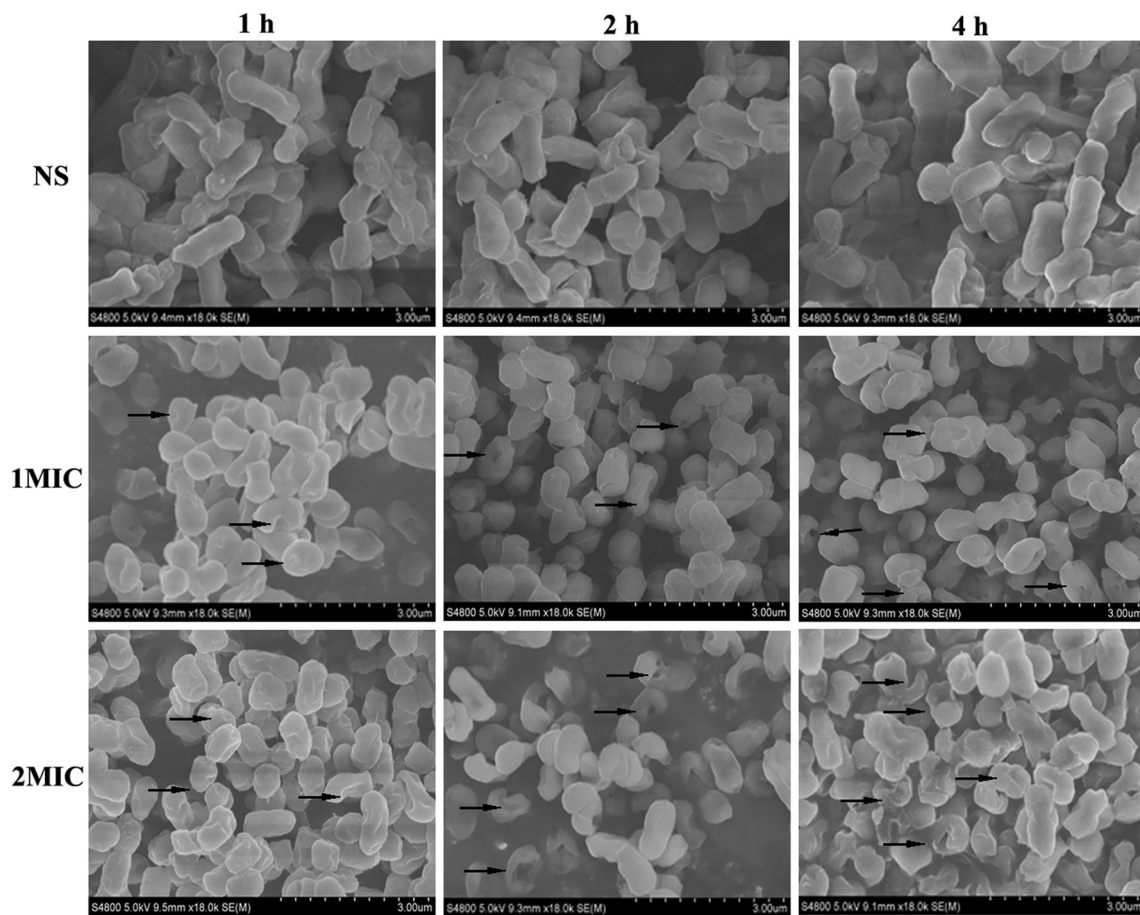


**Fig. 6** SEM observation of KP cells treated with PLA. The cells were treated with NS, 1 × MIC and 2 × MIC of PLA at 37 °C with shaking for 1 h, 2 h, and 4 h. The treated cells were fixed with glutaraldehyde,

dehydrated with a graded series of ethanol solutions, and then freeze-dried prior to gold sputtering for SEM analysis

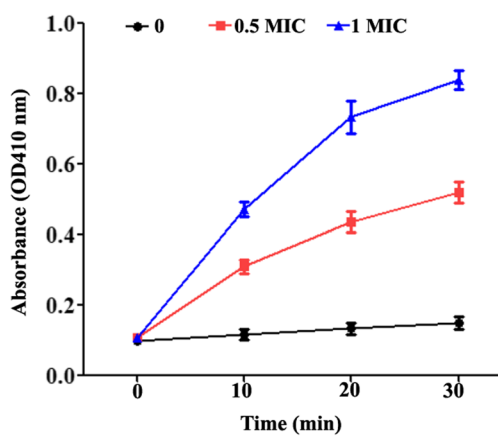


**Fig. 7** The leakage of AKP from the periplasmic space between the cell membrane and cell wall of KP treated with PLA or left untreated during incubation at 37°C for the indicated time. A KP cell suspension with a density of 1 × 10<sup>6</sup> CFU/mL as treated with 0 (sterile water), 0.5 × MIC, and 1 × MIC of PLA, respectively. The data are displayed as the means ± SD

the cells were stained with PI after treatment with 1 × MIC for 2 h, which increased to 90.3% with 2 × MIC, compared to only 5.3% in the control (Fig. 8b). These results show that a high concentration of PLA could rapidly destroy the integrity of the KP cell membrane.

**PLA could bind to and degrade genomic DNA of KP**

The interaction of PLA with bacterial genomic DNA was investigated by fluorescence spectroscopy. As shown in Fig. 9a, the addition of PLA to genomic DNA resulted in obvious fluorescence quenching, and the quenching intensity was positively correlated with the concentration of PLA. In addition, the effect of PLA on genomic DNA was observed by agarose gel electrophoresis. As shown in Fig. 9b, compared with untreated genomic DNA, the bands became more mobile in the gel after incubation with PLA, indicating DNA degradation that resulted in a smaller average molecular weight of the fragments. Moreover, the degradation became more pronounced with the increase of PLA concentration.

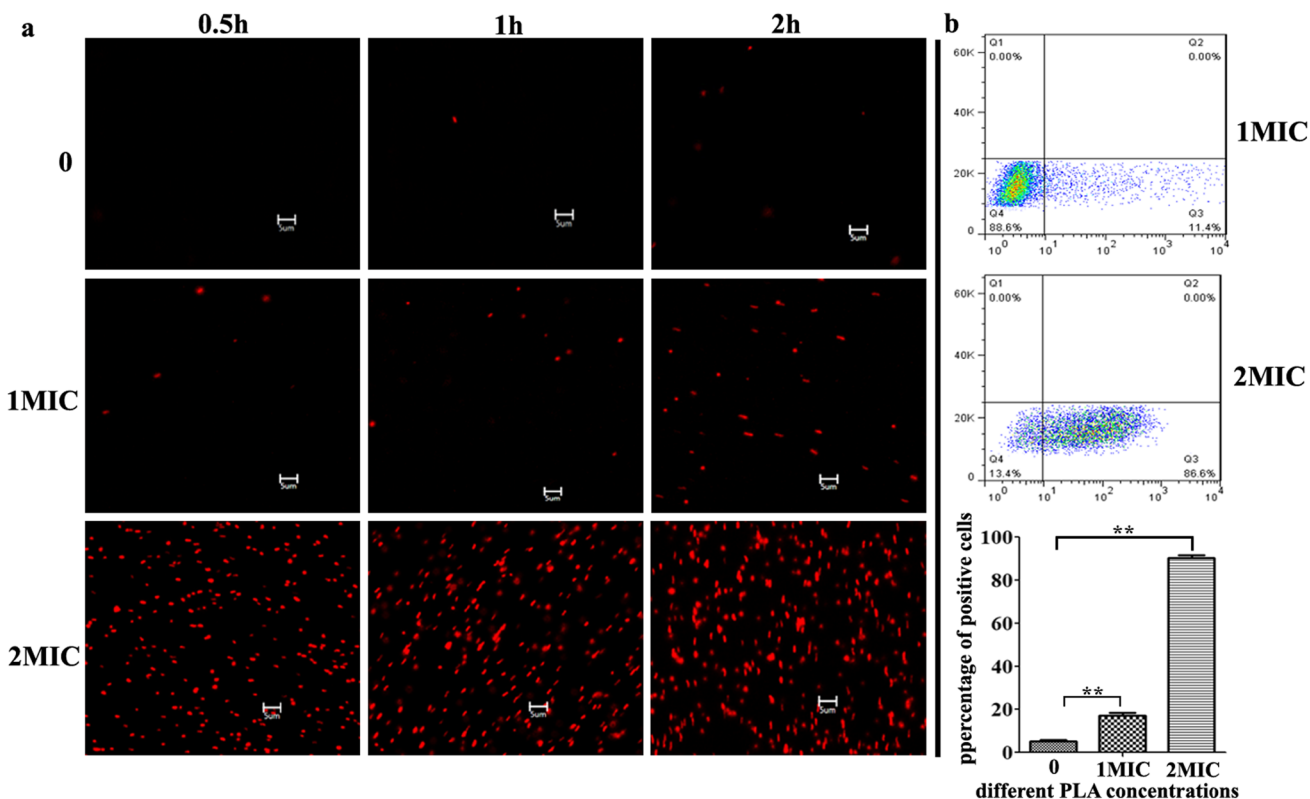


**Fig. 8** Effect of PLA on the membrane integrity of KP cells was determined by propidium iodide (PI) staining combined with fluorescence microscopy and flow cytometry analysis. **a** PI staining of KP cells treated with PLA for 0.5 h, 1 h, and 2 h at the concentration of

0, 1 ×, and 2 × MIC, respectively. Bar = 5 μm. **b** Quantification of PI-positive KP cells after treatment with the indicated concentrations of PLA for 2 h by flow cytometry

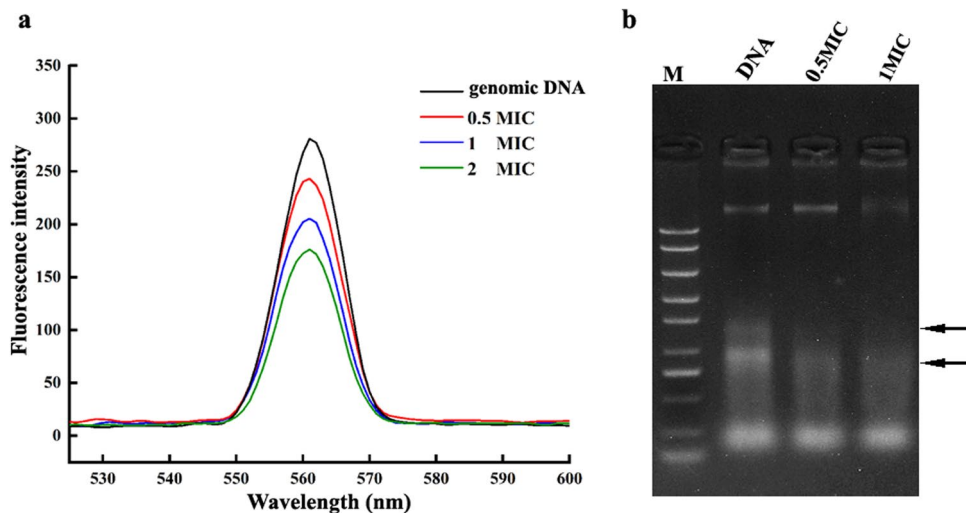


**Fig. 9** Detection of PLA binding to genomic DNA by fluorescence spectroscopy and agarose gel electrophoresis. **a** Bacterial genomic DNA was resuspended at a final concentration of 60 mg/L. Nucleic acid dye was added to the PLA-DNA mixture and incubated at 37 °C for 15 min, after which the fluorescence spectra were recorded. **b**

Genomic DNA was incubated with different concentrations of PLA (0, 0.5 × MIC, and 1 × MIC) at 37 °C for 15 min, after which 5 μL of the mixture was subjected to electrophoresis. M: DNA marker; the arrow indicates the degradation or disappearance of the corresponding nucleic acid band



These results indicated that PLA could bind to genomic DNA and promote its degradation.

## Discussion

Due to the increasing antibiotic resistance of KP, it is essential to find an antibiotic substitute for the treatment of KP infection for animals. In this study, we explored the antibacterial effect of PLA on KP and investigated the underlying mechanism.

The diameter of the inhibition zone (IZ), which directly reflects the antibacterial activity of PLA, was approximately 20 mm with all three tested strains, indicating that PLA has the inhibition effect on the KP (Fig. 1a). The MIC of PLA against KP was 2.5 mg/mL, which was similar with the MIC of PLA against *Escherichia coli* [13]. Notably, this was lower than the MIC of common antibiotics against KP, such as ceftriaxone, levofloxacin, gentamycin, and imipenem reported in another study [28]. The antibacterial effect of PLA *in vivo* lays an important foundation for its potential future application in veterinary medicine. In the mouse infection model, we found that PLA could significantly increase the survival rate of infected mice and ameliorate the pathological damage (Figs. 4 and 5). Notably, the protective effect of PLA in mice infected with KP was better than that of ceftazidime-avibactam [23]. However, this advantage may be since the Y8 strain used in the animal infection model in the previous study may be more virulent than the CVCC4080 strain used in our study. Early studies have reported that PLA may exert some positive effects on the immune system of laying hens and effectively improve their production performance and egg quality. In addition, it was found to potentially reduce *Escherichia coli* numbers in weanling and growing pigs [29, 30]. Moreover, the antibacterial effect of PLA is not affected by high temperature (Fig. S1). According to advantages of PLA with against harmful bacteria, improving of animal growth performance and high temperature resistance, it was suggested that the PLA has the great potential as the feed antibiotics substitute. However, the use of PLA as a feed additive needs to be reconsidered, since its inhibitory effect on *Escherichia coli* implies that it may impact the normal intestinal flora of animals. Therefore, if PLA is used as a feed additive, it should only be used when the animals exhibit symptoms of bacterial infection. Furthermore, the exact dosages of PLA in feeds for different animals need to be further explored. Furthermore, the low-cost and green technology for PLA production needs to be developed in industrial application [31].

According to the morphological and ultrastructural changes of KP, there was no fragmentation or cell lysis, but the cells first exhibited a rounded and wrinkled shape, while obvious local ruptures and pores could be observed on the

surface of the cells after prolonged treatment (Fig. 6). However, it was different from that of perilla rosmarinic acid, which directly destroyed the whole cell structure without changing the cell size [32]. While, the concave collapsed indentations and gaps observed indicated that the permeability of the cytoplasmic membrane was increased, leading to the formation of local pores, which directly resulted in the loss of viability. This phenomenon was different from that of *Escherichia coli* with no obvious broken and rupture cells, even treated with high concentration of PLA ( $2 \times$  MIC), which could be possibly attributed to the differences in cell membrane structure and composition [13]. Normally, bacterial AKP is located between the cell wall and the cell membranes. Accordingly, the activity of this enzyme will not be detected in the extracellular environment unless the bacterial cell wall is disrupted [33]. PLA destroyed the cell wall integrity of KP, resulting in leakage of AKP into the cell supernatant (Fig. 7). Propidium iodide (PI) can only penetrate cells with destroyed membranes and bind to nucleic acids. PI staining (Fig. 8) indicated that the effect of PLA against KP is similar to the effect of lactic acid, which can also damage the cell membrane integrity of bacteria [34]. However, differed from other organic acids (i.e., acetic acid, lactic acid), PLA has amphiphilic properties due to its hydrophobic benzene ring and hydrophilic carboxy group. Thus, it can more easily interact with lipids and proteins in the cell membrane to disrupt its integrity and increase its permeability [13].

In addition, it was speculated that PLA might penetrate cell membranes to interact with genomic DNA. DNA is the main carrier of genetic information, and the disruption of DNA generally results in cell death [13]. According to fluorescence spectroscopy and agarose gel electrophoresis, PLA was able to bind to genomic DNA of KP and induce its degradation (Fig. 9). Furthermore, SDS-PAGE result shown the number and brightness of protein bands decreased significantly when the cells were treated with  $1 \times$  MIC of PLA and confirmed that PLA at the minimum inhibitory concentration inhibits the synthesis of certain proteins in KP (Fig. S2). Above data demonstrated that genomic DNA is one of the key target molecules of PLA against KP. This result provided a different perspective for the further study of the antibacterial mechanism of PLA interaction with DNA. Although the results of gel electrophoresis could not illustrate how phenyllactic acid binds to DNA. According to previous studies on the binding of small molecules to DNA, it is speculated that the binding mode of phenyllactic acid to DNA is electrostatic and intercalation [35, 36].

In conclusion, the KP was sensitive to PLA with the MIC of 2.5 mg/mL. In the animal infection model, PLA dramatically increased the survival rate of infected mice and reduced the pathological damage to tissues. Furthermore, basing on the detected morphological changes, leakage of AKP, PI

staining suggested that the cellular wall membrane might be the target of PLA. Additional findings revealed that binding to bacterial genomic DNA may be another antibacterial mode of action of PLA. It was speculated that PLA could rapidly disrupt the integrity of KP cell membrane, enter the cells, bind to genomic DNA, and inhibit the expression of proteins necessary for the growth of KP. This study identified antibacterial characteristics and the molecular target of PLA action in KP, which provides a theoretical basis for the application of PLA as a potential antibiotic substitute for the treatment of KP infection in the veterinary field.

**Supplementary Information** The online version contains supplementary material available at <https://doi.org/10.1007/s42770-023-01126-8>.

**Funding** This study was supported by Zhejiang Provincial Natural Science Foundation of China (Grant No. LTGN23C180001), Science and Technology Plan Project of Taizhou (Grant No. 22nya08), and National College Students Innovation and Entrepreneurship Program (Grant No. 202210350030).

**Data availability** All data analyzed during this study are included in this published article. The raw data of this study are available from the author Gaowei Hu upon reasonable request.

## Declarations

**Ethics approval** All study procedures were approved by the Animal Care and Use Committee of Taizhou University (Approval No. TZXY-2022-20221046) and were in accordance with the “Zhejiang province animal use nursing ethics guide” (Zhejiang, China).

**Consent for publication** All authors consent for publication.

**Conflict of interest** The authors declare no competing interests.

## References

- Hu Y, Anes J, Devineau S, Fanning S (2021) *Klebsiella pneumoniae*: prevalence, reservoirs, antimicrobial resistance, pathogenicity, and infection: a hitherto unrecognized zoonotic bacterium. *Foodborne Pathog Dis* 18(2):63–84. <https://doi.org/10.1089/fpd.2020.2847>
- Marques C, Menezes J, Belas A, Aboim C, Cavaco-Silva P, Trigueiro G, Telo Gama L, Pomba C (2019) *Klebsiella pneumoniae* causing urinary tract infections in companion animals and humans: population structure, antimicrobial resistance and virulence genes. *J Antimicrob Chemother* 74(3):594–602. <https://doi.org/10.1093/jac/dky499>
- Mobasser G, Thong KL, Teh CSJ (2021) Genomic analysis revealing the resistance mechanisms of extended-spectrum beta-lactamase-producing *Klebsiella pneumoniae* isolated from pig and humans in Malaysia. *Int Microbiol* 24(2):243–250. <https://doi.org/10.1007/s10123-021-00161-5>
- Zou LK, Wang HN, Zeng B, Zhang AY, Li JN, Li XT, Tian GB, Wei K, Zhou YS, Xu CW et al (2011) Phenotypic and genotypic characterization of beta-lactam resistance in *Klebsiella pneumoniae* isolated from swine. *Vet Microbiol* 149(1–2):139–146. <https://doi.org/10.1016/j.vetmic.2010.09.030>
- Yang Y, Zhang A, Lei C, Wang H, Guan Z, Xu C, Liu B, Zhang D, Li Q, Jiang W et al (2015) Characteristics of plasmids cohabiting 16S rRNA methylases, CTX-M, and virulence factors in *Escherichia coli* and *Klebsiella pneumoniae* isolates from chickens in China. *Foodborne Pathog Dis* 12(11):873–880. <https://doi.org/10.1089/fpd.2015.2025>
- Chen CM, Tang HL, Chiou CS, Tung KC, Lu MC, Lai YC (2021) Colonization dynamics of *Klebsiella pneumoniae* in the pet animals and human owners in a single household. *Vet Microbiol* 256:109050. <https://doi.org/10.1016/j.vetmic.2021.109050>
- Petersen A, Aarestrup FM, Olsen JE (2009) The *in vitro* fitness cost of antimicrobial resistance in *Escherichia coli* varies with the growth conditions. *FEMS Microbiol Lett* 299(1):53–59. <https://doi.org/10.1111/j.1574-6968.2009.01734.x>
- Wang G, Zhao G, Chao X, Xie L, Wang H (2020) The characteristic of virulence, biofilm and antibiotic resistance of *Klebsiella pneumoniae*. *Int J Environ Res Public Health* 17(17). <https://doi.org/10.3390/ijerph17176278>
- Yang F, Deng B, Liao W, Wang P, Chen P, Wei J (2019) High rate of multidrug-resistant *Klebsiella pneumoniae* from human and animal origin. *Infect Drug Resist* 12:2729–2737. <https://doi.org/10.2147/IDR.S219155>
- Durdu B, Hakyemez IN, Bolukcu S, Okay G, Gultepe B, Aslan T (2016) Mortality markers in nosocomial *Klebsiella pneumoniae* bloodstream infection. *Springerplus* 5(1):1892. <https://doi.org/10.1186/s40064-016-3580-8>
- de Souza CM, da Silva AP, Junior NGO, Martínez OF, Franco OL (2022) Peptides as a therapeutic strategy against *Klebsiella pneumoniae*. *Trends Pharmacol Sci* 43(4):335–348. <https://doi.org/10.1016/j.tips.2021.12.006>
- Wang F, Wu H, Jin P, Sun Z, Liu F, Du L, Wang D, Xu W (2018) Antimicrobial activity of phenyllactic acid against *Enterococcus faecalis* and its effect on cell membrane. *Foodborne Pathog Dis* 15(10):645–652. <https://doi.org/10.1089/fpd.2018.2470>
- Ning Y, Yan A, Yang K, Wang Z, Li X, Jia Y (2017) Antibacterial activity of phenyllactic acid against *Listeria monocytogenes* and *Escherichia coli* by dual mechanisms. *Food Chem* 228:533–540. <https://doi.org/10.1016/j.foodchem.2017.01.112>
- Mu W, Yu S, Zhu L, Zhang T, Jiang B (2012) Recent research on 3-phenyllactic acid, a broad-spectrum antimicrobial compound. *Appl Microbiol Biotechnol* 95(5):1155–1163. <https://doi.org/10.1007/s00253-012-4269-8>
- Sorrentino E, Tremonte P, Succi M, Iorizzo M, Pannella G, Lombardi SJ, Sturchio M, Coppola R (2018) Detection of antilisterial activity of 3-phenyllactic acid using *Listeria innocua* as a model. *Front Microbiol* 9:1373. <https://doi.org/10.3389/fmicb.2018.01373>
- Chatterjee M, D'Morris S, Paul V, Warriar S, Vasudevan AK, Vanuopadath M, Nair SS, Paul-Prasanth B, Mohan CG, Biswas R (2017) Mechanistic understanding of phenyllactic acid mediated inhibition of quorum sensing and biofilm development in *Pseudomonas aeruginosa*. *Appl Microbiol Biotechnol* 101(22):8223–8236. <https://doi.org/10.1007/s00253-017-8546-4>
- Bernardini A, Cuesta T, Tomas A, Bengoechea JA, Martinez JL, Sanchez MB (2019) The intrinsic resistome of *Klebsiella pneumoniae*. *Int J Antimicrob Agents* 53(1):29–33. <https://doi.org/10.1016/j.ijantimicag.2018.09.012>
- Guo W, Shan K, Xu B, Li J (2015) Determining the resistance of carbapenem-resistant *Klebsiella pneumoniae* to common disinfectants and elucidating the underlying resistance mechanisms. *Pathog Glob Health* 109(4):184–192. <https://doi.org/10.1179/204773215Y.0000000022>
- Rasheed JK, Anderson GJ, Yigit H, Queenan AM, Domenech-Sanchez A, Swenson JM, Biddle JW, Ferraro MJ, Jacoby GA, Tenover FC (2000) Characterization of the extended-spectrum beta-lactamase reference strain, *Klebsiella pneumoniae* K6

- (ATCC 700603), which produces the novel enzyme SHV-18. *Antimicrob Agents Chemother* 44(9):2382–2388. <https://doi.org/10.1128/AAC.44.9.2382-2388.2000>
20. Liang W, Li H, Zhou H, Wang M, Zhao X, Sun X, Li C, Zhang X (2021) Effects of Taraxacum and Astragalus extracts combined with probiotic *Bacillus subtilis* and *Lactobacillus* on *Escherichia coli*-infected broiler chickens. *Poult Sci* 100(4):101007. <https://doi.org/10.1016/j.psj.2021.01.030>
  21. Tran HNH, Graham L, Adukwu EC (2020) *In vitro* antifungal activity of Cinnamomum zeylanicum bark and leaf essential oils against *Candida albicans* and *Candida auris*. *Appl Microbiol Biotechnol* 104(20):8911–8924. <https://doi.org/10.1007/s00253-020-10829-z>
  22. Espinel-Ingroff A, Chaturvedi V, Fothergill A, Rinaldi MG (2002) Optimal testing conditions for determining MICs and minimum fungicidal concentrations of new and established antifungal agents for uncommon molds: NCCLS collaborative study. *J Clin Microbiol* 40(10):3776–3781. <https://doi.org/10.1128/JCM.40.10.3776-3781.2002>
  23. Zhang W, Guo Y, Li J, Zhang Y, Yang Y, Dong D, Zhu D, He P, Hu F (2018) *In vitro* and *in vivo* bactericidal activity of ceftazidime-avibactam against Carbapenemase-producing *Klebsiella pneumoniae*. *Antimicrob Resist Infect Control* 7:142. <https://doi.org/10.1186/s13756-018-0435-9>
  24. Qian W, Sun Z, Wang T, Yang M, Liu M, Zhang J, Li Y (2020) Antimicrobial activity of eugenol against carbapenem-resistant *Klebsiella pneumoniae* and its effect on biofilms. *Microb Pathog* 139:103924. <https://doi.org/10.1016/j.micpath.2019.103924>
  25. Liu F, Sun Z, Wang F, Liu Y, Zhu Y, Du L, Wang D, Xu W (2020) Inhibition of biofilm formation and exopolysaccharide synthesis of *Enterococcus faecalis* by phenyllactic acid. *Food Microbiol* 86:103344. <https://doi.org/10.1016/j.fm.2019.103344>
  26. Garcia-Heredia A, Garcia S, Merino-Mascorro JA, Feng P, Heredia N (2016) Natural plant products inhibits growth and alters the swarming motility, biofilm formation, and expression of virulence genes in enteroaggregative and enterohemorrhagic *Escherichia coli*. *Food Microbiol* 59:124–132. <https://doi.org/10.1016/j.fm.2016.06.001>
  27. Song X, Li R, Zhang Q, He S, Wang Y (2022) Antibacterial effect and possible mechanism of salicylic acid microcapsules against *Escherichia coli* and *Staphylococcus aureus*. *Int J Environ Res Public Health* 19(19). <https://doi.org/10.3390/ijerph191912761>
  28. Lou W, Venkataraman S, Zhong G, Ding B, Tan JPK, Xu L, Fan W, Yang YY (2018) Antimicrobial polymers as therapeutics for treatment of multidrug-resistant *Klebsiella pneumoniae* lung infection. *Acta Biomater* 78:78–88. <https://doi.org/10.1016/j.actbio.2018.07.038>
  29. Wang JP, Yoo JS, Lee JH, Jang HD, Kim HJ, Shin SO, Seong SI, Kim IH (2009) Effects of phenyllactic acid on growth performance, nutrient digestibility, microbial shedding, and blood profile in pigs. *J Anim Sci* 87(10):3235–3243. <https://doi.org/10.2527/jas.2008-1555>
  30. Wang JP, Lee JH, Yoo JS, Cho JH, Kim HJ, Kim IH (2010) Effects of phenyllactic acid on growth performance, intestinal microbiota, relative organ weight, blood characteristics, and meat quality of broiler chicks. *Poult Sci* 89(7):1549–1555. <https://doi.org/10.3382/ps.2009-00235>
  31. Wu H, Guang C, Zhang W, Mu W (2023) Recent development of phenyllactic acid: physicochemical properties, biotechnological production strategies and applications. *Crit Rev Biotechnol* 43(2):293–308. <https://doi.org/10.1080/07388551.2021.2010645>
  32. Zhang J, Cui X, Zhang M, Bai B, Yang Y, Fan S (2022) The antibacterial mechanism of perilla rosmarinic acid. *Biotechnol Appl Biochem* 69(4):1757–1764. <https://doi.org/10.1002/bab.2248>
  33. Wang JY, Zhang WJ, Tang CE, Xiao J, Xie BJ, Sun ZD (2018) Synergistic effect of B-type oligomeric procyanidins from lotus seedpod in combination with water-soluble Poria cocos polysaccharides against *E-coli* and mechanism. *J Funct Foods* 48:134–143. <https://doi.org/10.1016/j.jff.2018.07.015>
  34. Wang CJ, Chang T, Yang H, Cui M (2015) Antibacterial mechanism of lactic acid on physiological and morphological properties of *Salmonella Enteritidis*, *Escherichia coli* and *Listeria monocytogenes*. *Food Control* 47:231–236. <https://doi.org/10.1016/j.foodcont.2014.06.034>
  35. Huang R, Wang LR, Guo LH (2010) Highly sensitive electrochemiluminescence displacement method for the study of DNA/small molecule binding interactions. *Anal Chim Acta* 676(1–2):41–45. <https://doi.org/10.1016/j.aca.2010.07.033>
  36. Brudzynski K, Abubaker K, Miotto D (2012) Unraveling a mechanism of honey antibacterial action: polyphenol/H(2)O(2)-induced oxidative effect on bacterial cell growth and on DNA degradation. *Food Chem* 133(2):329–336. <https://doi.org/10.1016/j.foodchem.2012.01.035>
- Publisher's Note** Springer Nature remains neutral with regard to jurisdictional claims in published maps and institutional affiliations.
- Springer Nature or its licensor (e.g. a society or other partner) holds exclusive rights to this article under a publishing agreement with the author(s) or other rightsholder(s); author self-archiving of the accepted manuscript version of this article is solely governed by the terms of such publishing agreement and applicable law.